RSC Advances

PAPER

View Article Online
View Journal | View Issue

Cite this: *RSC Adv.*, 2017, **7**, 964

A colorimetric and fluorescent pH probe for imaging in *E. coli* cells†

Jianbin Chao,*[a] Kailun Song,[ab] Huijuan Wang,[ab] Zhiqing Li,[ab] Yongbin Zhang,[d] Caixia Yin,[c] Fangjun Huo,[d] Juanjuan Wang[a] and Ting Zhang[a]

Received 8th October 2016
Accepted 6th November 2016

DOI: 10.1039/c6ra24885c

www.rsc.org/advances

A colorimetric and fluorescent pH probe 1-(4-methylphenyl)-3-(4-dimethylaminophenyl) acrylketone (**MDAK**) was facilely prepared. The probe exhibited strong pH-dependent behavior and responded linearly and rapidly to minor pH fluctuations within the range of 1.53–3.96. In addition, **MDAK** displayed a notably large Stokes shift of 121 nm. **MDAK** possessed a highly selective response to H^+ over other metal ions, amion acids and displayed good photostability and excellent reversibility. Furthermore, it can be applied to visualize extreme acidity in *E. coli* cells.

1. Introduction

Intracellular pH plays a significant role in a mass of cellular events, including cell proliferation and apoptosis,[1–3] enzymatic activity,[4,5] endocytosis,[6] ion transport and homeostasis,[7,8] muscle contraction[9] and other cellular processes. The H^+ concentration is maintained within very narrow limits under normal physiological conditions. The normal value is about 40 nmol L^{-1} (pH 7.40) and varies by about 5 nmol L^{-1} (pH 7.35–7.45).[10] As an important indication of cellular health, slight changes of intracellular pH have a traumatizing effect on the progress of distinct pathophysiologic states and even cause cellular dysfunction which is closely related to many serious diseases, such as cancer, cardiopulmonary and Alzheimer's disease[11–13] (one of the neurodegenerative disorders). Hence, sensing and monitoring pH fluctuations in living cells is crucial for investigating cellular functions and further providing insight into physiological and pathological processes.

A range of analytical methods has been reported for the measurement of pH, such as microelectrodes,[14] nuclear magnetic resonance (NMR)[15] and molecular spectroscopy.[16–18] Among these methods, fluorescence spectroscopy has attracted much more attention due to its noninvasiveness, excellent sensitivity, fast response time, simple operation, high signal-to-noise ratio and the ability to continuously monitor the rapid kinetic pH changes.[19,20] Fluorescent probes, as the most important area of fluorescence spectroscopy, have been extensively used due to their high selectivity and sensitivity, unrivaled spatiotemporal resolution, convenient operation and possibility of real time monitoring.[21] Moreover, with the combination of fluorescent probes and confocal laser scanning microscopy, fluorescence imaging becomes one of the most powerful techniques for the continuous observation of dynamic biochemical and cellular processes of living systems.[22] Therefore, fluorescent probes with different design strategies continue to be developed.

In the past few years, a great deal of pH probes reported in literature can be broadly divided into two main classes: one type for cytosol that works in a pH region 6.8–7.4 (ref. 10, 19 and 23–26) and the other type for acidic organelles such as lysosomes and endosomes[21,27–35] which function at pH 4.5–6.0. However, the fluorescent probes for extreme acidity (pH < 4)[36–41] were paid relatively less attention. In some eukaryotic cells, acidic pH has important effect on organelles along the secretory and endocytic pathways.[42] Stomach, which contains gastric acid with acidity pH 2.0–3.0, is the strongly acidic organ of human beings.[41] Gastric acid plays an important role in the physiological processes. In the stomach, gastric acid can activate pepsinogen into pepsin which decompose the protein of food,[43–45] and provide a suitable acid condition for the activity of pepsin. Also, the extreme acidic environment can kill bacteria in the water and food. In addition, as the gastric acid into the small intestine, it will indirectly promote the secretion of bile and pancreatic juice, and accelerate the absorption of iron and calcium. Abnormal pH values of gastric acid influences the function of stomach, which will cause stomach disorders. In highly acidic conditions (pH < 4), most of the living species could hardly live, but a great number of microorganisms such as acidophiles and *Helicobacter pylori* can live under such extreme conditions.[46,47] Furthermore, enteric bacteria such as *Escherichia coli* and *Salmonella* species survive through the highly acidic mammalian stomach.[47,48]

[a]*Scientific Instrument Center, Shanxi University, Taiyuan 030006, China. E-mail: chao@sxu.edu.cn; Fax: +86-351-721-2621; Tel: +86-351-721-2621*

[b]*School of Chemistry and Chemical Engineering, Shanxi University, Taiyuan 030006, China*

[c]*Institute of Molecular Science, Shanxi University, Taiyuan 030006, China*

[d]*Research Institute of Applied Chemistry, Shanxi University, Taiyuan 030006, China*

† Electronic supplementary information (ESI) available. See DOI: 10.1039/c6ra24885c

Thus, there is a great need in designing pH probes with high sensitivity, large Stokes shift, good photostability for extreme acidity.

In this paper, we reported a colorimetric and fluorescent pH probe 1-(4-methylphenyl)-3-(4-dimethylaminophenyl) acrylketone **MDAK**. **MDAK** not only showed high sensitivity, reversible response, and excellent stability, but also displayed a notably large Stokes shift of 121 nm which could reduce the excitation interference. The pH titration indicated that **MDAK** exhibited remarkable pH-dependent behavior in the fluorescence (λ_{ex} = 440 nm) with a pK_a value of 2.71. Furthermore, **MDAK** responded to pH fluctuations within a wider pH range (1.53–3.96). More importantly, the probe had been successfully used for fluorescence imaging in *E. coli* cells under extreme acidity conditions.

2. Experimental section

2.1. Materials and apparatus

Unless otherwise stated, all other reagents were purchased from commercial suppliers and applied directly without purification. Twice-distilled water was used in all the experiments. Fluorescence measurements were obtained with a Hitachi F-7000 fluorescence spectrophotometer. Photomultiplier (PMT) voltage was set at 600 V for the fluorescence spectra. Absorption spectra were measured with a UV-2450 spectrophotometer in a 4.5 mL (1 cm in diameter) cuvette with 2 mL solution. NMR spectra were recorded on a Bruker instrument (AVANCE|||HD) with TMS as the internal standard in DMSO-d_6 of 600 MHz for ^{1}H NMR and 150 MHz for ^{13}C NMR, respectively. Mass spectra were taken on a Thermo Scientific Q Exactive mass spectrometer. Fluorescent images were performed on a ZEISS LSM-880 confocal laser scanning microscope.

2.2. Synthesis and characterization of fluorescent probe

4-Dimethylaminobenzaldehyde (1.94 g, 13 mmol), 1-(4-methylphenyl)-ethanone (1.79 g, 13 mmol), 10% NaOH solution (3 mL), anhydrous ethanol (100 mL) were added in turn to a 250 mL flask. The reaction was stirred at room temperature for 4 h. The progress of reaction was monitored by thin-layer chromatography (trichloromethane : petroleum ether = 1 : 3). The mixture was subsequently filtered under reduced pressure. The crude product was recrystallized with anhydrous ethanol and dried overnight under a vacuum to obtain yellow solid (2.77 g, 85%). The synthesis route of **MDAK** was shown in Scheme 1. ^{1}H NMR δ/ppm (600 MHz, DMSO-d_6): 8.03 (d, J = 7.8 Hz, 2H), 7.71 (d, J = 8.4 Hz, 2H), 7.65 (t, J = 10.8 Hz, J = 15.6 Hz, 2H), 7.36 (d, J = 7.8 Hz, 2H), 6.75 (d, J = 8.4 Hz, 2H), 3.01 (s, 6H), 2.40 (s, 3H); ^{13}C NMR (150 MHz, DMSO-d_6): 188.58, 152.40, 145.27, 143.27, 136.26, 131.18, 129.68, 128.81, 122.52, 116.57, 112.21, 40.17, 21.62 (Fig. S1†). HRMS (ESI) calcd for $[M + H]^+$ 266.15394, found 266.15403 (Fig. S2†).

2.3. General UV-vis and fluorescence spectra measurement

Stock solution of probe (1.0 mM) was prepared in DMSO. The solution for spectroscopic determination was obtained by diluting the stock solution to 10 μM in DMSO/water (1/3 v/v) medium. The pH variations of the solution were adjusted by adding the different volumes of HCl (1.0 M, 0.1 M). Spectral data were recorded after each addition. The excitation and emission slit widths were 5 nm and 10 nm, respectively. All spectroscopic experiments were carried out at room temperature.

2.4. *E. coli* cells culture and imaging

According to the method reported in literature,[37] *E. coli* cells were incubated at 37 °C in Luria–Bertani (LB) culture medium (tryptone 10 g L^{-1}, yeast extract 5 g L^{-1}, and NaCl 10 g L^{-1}) for 17 h in a table concentrator at 180 rpm. Then the culture was centrifuged at 5000 rpm for 5 min to collect *E. coli* cells. The sediment was washed with sterile water and then resuspended in solutions of different pH (6.81, 2.70 and 1.22). Five minutes after resuspension, the probe dissolved in DMSO was added into every tube to a final probe concentration of 30 μM. *E. coli* cells with the probe were incubated in a table concentrator for 2 h and then smeared on slides and observed by confocal laser scanning microscope.

3. Results and discussion

3.1. UV-vis spectrum study

Fig. 1 showed the UV-vis absorption spectral change of **MDAK** at different pH values. As the pH decreased from 6.81 to 1.07, the absorbance at 437 nm reduced dramatically. Upon decreasing the pH from 6.81 to 3.40, the absorbance at 280 nm reduced gradually. When pH was less than 3.40, the absorption spectra exhibit a red shift from 280 to 300 nm and increased clearly. The observed absorption enhancement might be caused by experimental instrument. On this account, the absorption signals showed a sharp increase at about 360 nm for the systems with

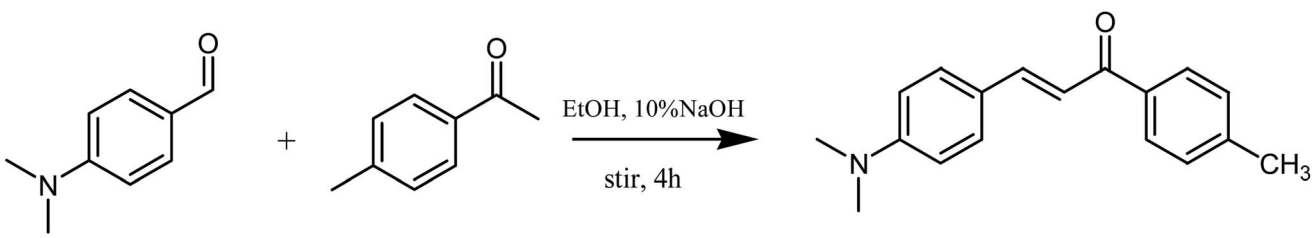

Scheme 1 Synthesis route of probe MDAK.

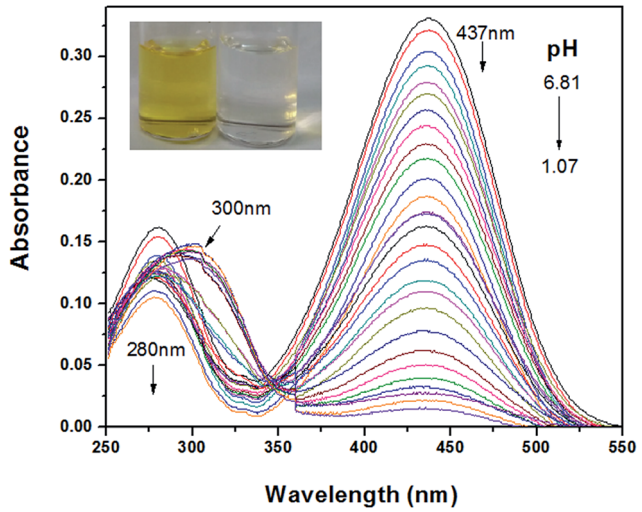

Fig. 1 The absorption spectra of MDAK as pH decreased from 6.81 to 1.07. Inset: the photograph of probe solution (10 μM) as pH increased from 6.81 to 1.07.

low pH values. At this wavelength, the spectrophotometer changed its light sources, which resulting in the increment of absorption signals at 300 nm. According to Fig. 1, the molar extinction coefficient of probe could be obtained by using Lambert–Beer's law: $\varepsilon = 3.31 \times 10^4$ L mol^{-1} cm^{-1} ($\lambda = 437$ nm, pH 6.81). In addition, a notable color change from yellow to colourless can be observed with pH decreasing, which proved that **MDAK** could serve as a visual probe for the determination of pH fluctuations.

3.2. Fluorescence spectrum study

Fluorescence pH titrations were performed in DMSO/water (1/3, v/v) at a probe concentration of 10 μM. As shown in Fig. 2a, in the absence of H^+, the probe solution exhibited an intense emission band centered at 561 nm ($\lambda_{ex} = 440$ nm) with a large Stokes shift of 121 nm. The large Stokes shift could help to reduce the excitation interference. With the variation of pH from 6.81 to 1.07, the probe showed turn-off fluorescence. Meanwhile, we could observed that the probe undergone distinct color change from bright yellow to nonfluorescence under UV lamp. Fig. 2b displayed the results of sigmoidal fitting of the pH-dependent emission at 561 nm, affording a pK_a value of 2.71. The emission intensity also showed good linearity with pH in the range 1.53–3.96, according to the linear regression equation $F = 443.51$ pH–575.83, with a linear coefficient of 0.9968 (inset of Fig. 2b). The data indicated that the probe could be used to detect pH quantitatively in extreme acidity.

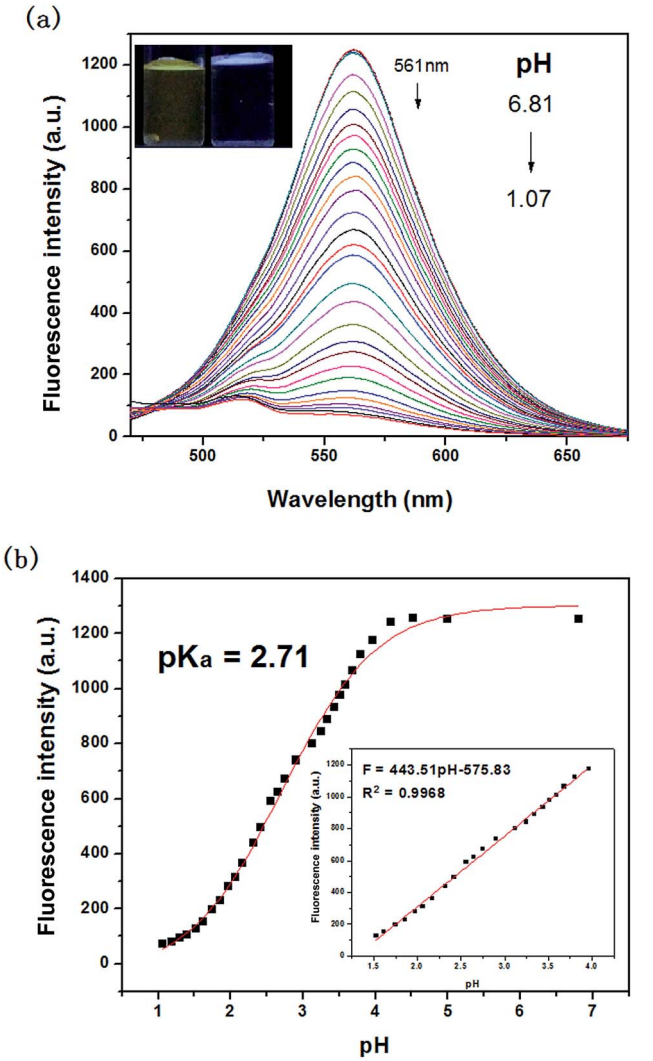

Fig. 2 (a) Fluorescence spectra of MDAK (10 μM) as pH decreased from 6.81 to 1.07. (λ_{ex} = 440 nm, slits: 5 nm/10 nm). Inset: the photograph of MDAK solution (10 μM) as pH decreased from 6.81 to 1.07 under a UV light. (b) Sigmoidal fitting of pH-dependent fluorescence intensity at 561 nm. Inset: the good linearity in the pH range of 1.53–3.96.

3.3. Selectivity study

To examine whether the probe could detect H^+ efficiently, the selectivity of **MDAK** (10 μM) to acidic pH over metal ions was investigated at pH 6.81 and 2.60 by competition experiments, respectively. Fig. 3 exhibited that in the presence of physiologically ubiquitous metal ions (K^+, Na^+, Ca^{2+} and Mg^{2+}) do not give any obvious emission change at the two pH values. Similarly, the addition of other metal cations, such as Zn^{2+}, Al^{3+}, Pb^{2+}, Mn^{2+}, Co^{2+}, Cr^{3+}, Hg^{2+}, Bi^{3+}, Ni^{2+}, Cu^{2+}, Fe^{2+}, Fe^{3+} caused no appreciable spectroscopic changes under the testing conditions. Furthermore, some amion acids (cysteine, alanine, leucine, glycine, glutamate and histidine) exhibited negligible effect. The results suggested that the probe showed excellent selectivity toward H^+ over metal cations and some amion acids.

3.4. Photostability and reversibility study

The stability of the probe was tested by measuring the fluorescent response during 2 h. Fig. 4a showed the time course of fluorescence intensity of **MDAK** (10 μM) at pH 3.96, 2.75, and 1.53 at room temperature, which proved that the probe could

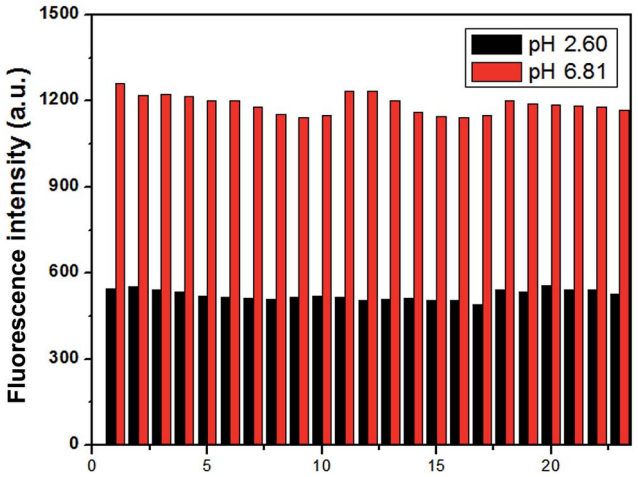

Fig. 3 Fluorescence intensity of 10 μM **MDAK** in DMSO/water (1/3 v/v) at pH 6.81 and 2.60 in the presence of diverse metal ions and amion acids: (1) blank; (2) 50 mM K^+; (3) 50 mM Na^+; (4) 5 mM Ca^{2+}; (5) 0.2 mM Zn^{2+}; (6) 0.2 mM Mg^{2+}; (7) 0.1 mM Al^{3+}; (8) 0.1 mM Pb^{2+}; (9) 0.1 mM Mn^{2+}; (10) 0.1 mM Co^{2+}; (11) 0.1 mM Cr^{3+}; (12) 0.1 mM Hg^{2+}; (13) 50 μM Bi^{3+}; (14) 0.1 mM Ni^{2+}; (15) 0.1 mM Cu^{2+}; (16) 0.1 mM Fe^{2+}; (17) 0.1 mM Fe^{3+}; (18) 0.1 mM cysteine; (19) 0.1 mM alanine; (20) 0.1 mM leucine; (21) 0.1 mM glycine; (22) 0.1 mM glutamate; (23) 0.1 mM histidine (λ_{ex} = 440 nm).

instantly respond to the change of H^+ concentration. The experimental results proved that the probe possessed good photostability.

It is well-known that the reversibility of pH probe is highly required. Therefore, we explored the reversibility of **MDAK**. The pH value of the solution was switched back and forth between 6.81 and 1.22 by using concentrated hydrochloric acid and aqueous sodium hydroxide. Fig. 4b clearly revealed that the probe exhibited a highly reversible response to pH and the response times in different pH values were less than 1 s. Switching between the fluorescence on/off states could thus be repeated accompanied with the color change repeatedly between yellow (pH 6.81) and colorless (pH 1.22), which enabled us to propose a mechanism for the equilibrium of probe with variations of pH (Scheme 2).

3.5. ^{1}H NMR analysis

^{1}H NMR experiments were carried out to explore the changes of protons. As shown in Fig. 5, the chemical shift values of H-a, H-b, H-c shifted downfield, whereas the other protons experienced only a small shift. At acidic condition, the N atom of **MDAK** was protonated to generated N^+. The N^+ possessed stronger electro-withdrawing ability than N, so the proton signals (H-a, at δ 3.01) of the methyl group connected with N were significantly shifted downfield to δ 3.08 under acidic condition. The similar results were obtained for the proton signals (H-b, H-c) of the phenyl group connected with N. Therefore, H was added to the N atom of **MDAK**.

3.6. Theoretical calculations

To better understand the optical responses of **MDAK** upon binding with H^+, time-dependent density functional theory

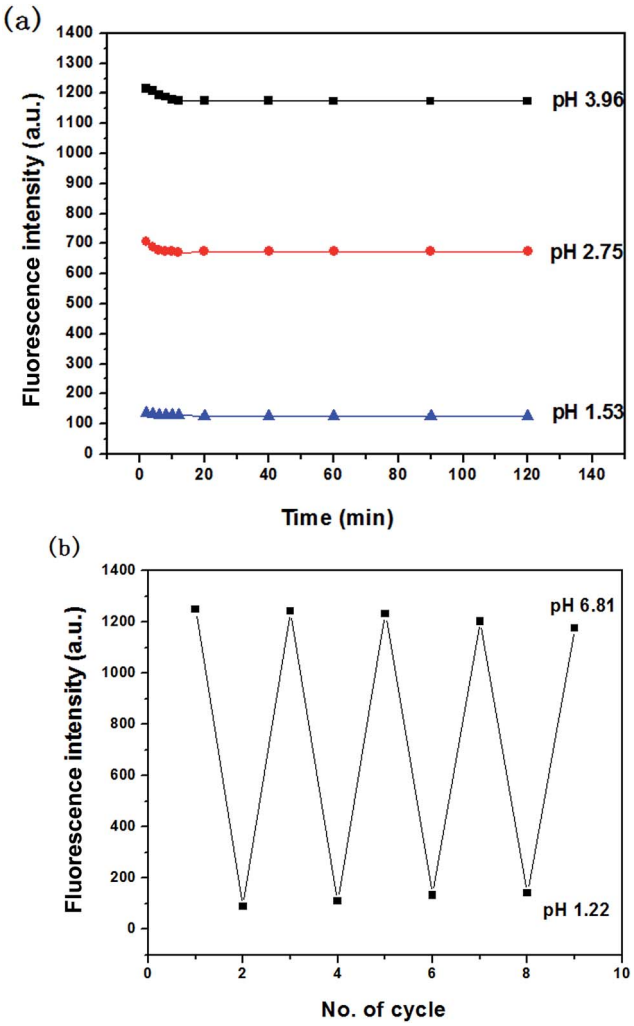

Fig. 4 (a) Changes in fluorescence intensity at 561 nm for **MDAK** (10 μM) in DMSO/water (1/3, v/v) system with times at pH 3.96, 2.75, 1.53, respectively. (b) Reversibility of the fluorescence response at 561 nm of **MDAK** (10 μM) between pH 6.81 and 1.22 (λ_{ex} = 440 nm).

(TD-DFT) calculations were performed using Gaussian 09 program. The ground state geometries were optimized by using B3LYP functional with 6-31+G (d) basis set. Fig. 6 displayed the optimized structures, the lowest unoccupied, the highest occupied molecular orbital (LUMO and HOMO) plots of **MDAK** and its protonated forms in ground state. From Fig. 6 we could see that the HOMO of **MDAK** located on the p orbits of N and C at the left side of the molecule, and the LUMO of **MDAK** located on the p orbits of N and C of the molecule. However, the HOMO of **MDAK**-H^+ located on the p orbits of C at the right side, which are far away from the N atoms, and the LUMO of **MDAK**-H^+ located on the p orbits of C of the molecule. To sum up, the protonation affected the distribution of the frontier molecular orbitals.

3.7. Imaging for *E. coli* cells

Encouraged by the above results, we next investigated whether the probe could be used to monitor pH changes in living

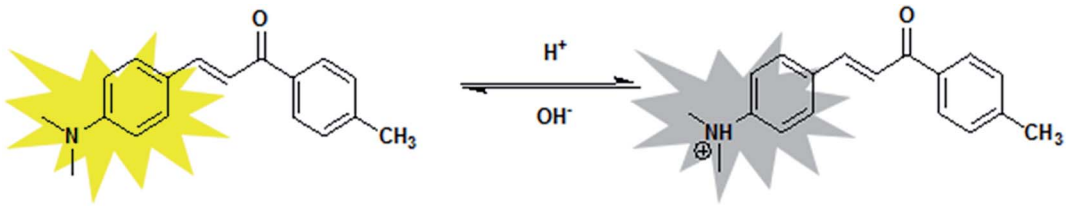

Scheme 2 The acid–base form equilibrium of MDAK.

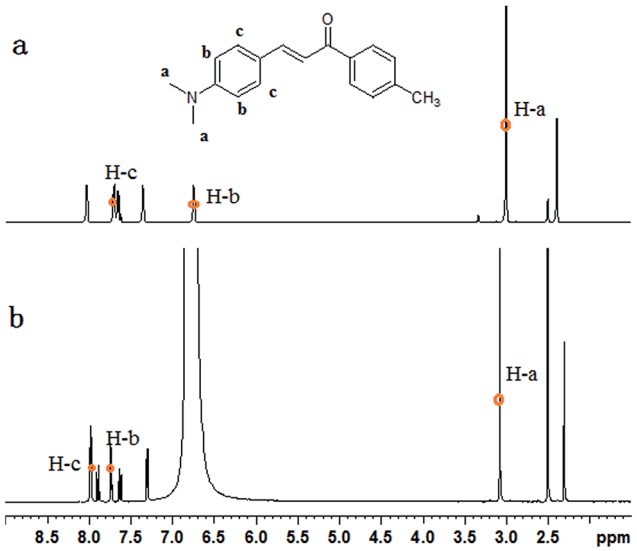

Fig. 5 ^{1}H NMR spectra of MDAK in DMSO-d_6 before (a) and after (b) the addition of hydrochloric acid.

samples. We used *E. coli* cells as a model to study the fluorescence change of *E. coli* cells incubated with probe (30 μM) under different pH conditions using confocal laser scanning microscope (Fig. 7). The yellow fluorescence (485–600 nm) was captured by 458 nm laser. It can be seen that the *E. coli* cells

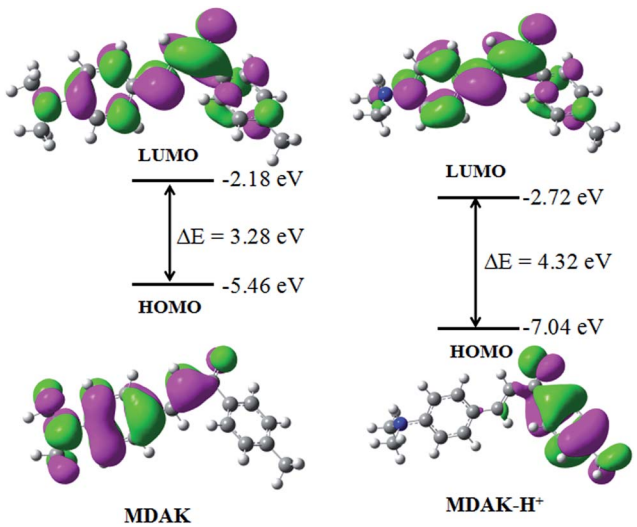

Fig. 6 Calculated LUMO and HOMO distributions of MDAK and its protonated products MDAK-H$^+$.

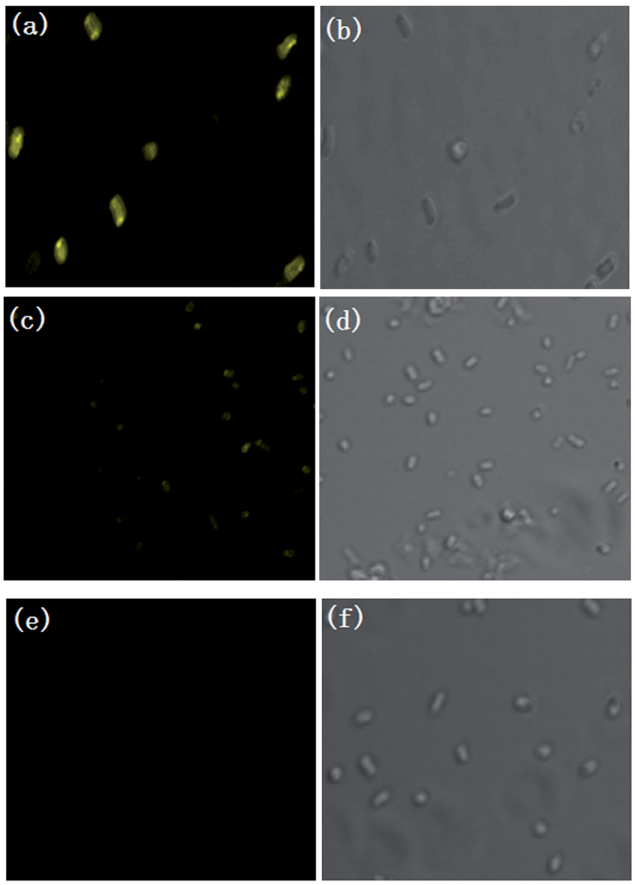

Fig. 7 Confocal fluorescence images of 30 μM MDAK in *E. coli* cells at pH 6.81 (a, b), 2.70 (c, d), and 1.22 (e, f). (b, d and f) Bright-field image of panel (a, c and e), respectively. Excitation wavelength was 458 nm, and emission was collected in the yellow channel (485–600 nm).

displayed bright yellow fluorescence (Fig. 7a) at pH 6.81. The yellow fluorescence intensity dropped sharply with the pH decreasing to 2.70 (Fig. 7c), and almost no fluorescence was observed as the pH decreased to 1.22 (Fig. 7e). The results confirmed that the probe was able to image pH changes under extreme acidity in *E. coli* cells and we believed that it may be applied to other biological systems with extreme acidity conditions.

4. Conclusion

In summary, a pH probe **MDAK** was easily synthesized in a one-step reaction. As the pH decreased from 6.81 to 1.07, the

fluorescence intensity at 561 nm reduced dramatically. A pK_a value of 2.71 and a good linearity relation in the pH range of 1.53–3.96 indicated that the probe could be used in quantitative measuring pH under extreme acidity. The fluorescence imaging confirmed that the probe could monitor pH fluctuations in *E. coli* cells under extreme acidity. The large Stokes shift, highly selectivity, good photostability and excellent reversibility of the probe demonstrated that it may act as an effective intracellular pH imaging agent under extreme acidity conditions in the biomedical and biological fields.

Acknowledgements

The work was supported by the National Natural Science Foundation of China (No. 21472118), the Shanxi Province Science Foundation for Youths (No. 2012021009-4 and 2013011011-1), the Shanxi Province Foundation for Returnee (No. 2012-007), the Taiyuan Technology Star Special (No. 12024703), the Program for the Top Young and Middle-aged Innovative Talents of Higher Learning Institutions of Shanxi (TYMIT, No. 2013802), Talents Support Program of Shanxi Province (No. 2014401) and Shanxi Province Outstanding Youth Fund (No. 2014021002), the Scientific and Technological Innovation Programs of Higher Education Institutions in Shanxi (20111001), and the Shanxi Province Foundation for College Students of Science and Technology Innovation projects (No. 2013328).

Notes and references

1 S. Humez, M. Monet, F. Coppenolle, P. Delcourt and N. Prevarskaya, *Am. J. Physiol.: Cell Physiol.*, 2004, **287**, 1733.
2 D. Pérez-Sala, D. Collado-Escobar and F. Mollinedo, *J. Biol. Chem.*, 1995, **270**, 6235.
3 R. A. Gottlieb, J. Nordberg, E. Skowronski and B. M. Babior, *Proc. Natl. Acad. Sci. U. S. A.*, 1996, **93**, 654.
4 R. Tsuboi, I. Ko, K. Takamori and H. Ogawa, *Infect. Immun.*, 1989, **57**, 3479.
5 R. T. Kennedy, L. Huang and C. A. Aspenwall, *J. Am. Chem. Soc.*, 1996, **118**, 1795.
6 M. Lakadamyali, M. J. Rust, H. P. Babcock and X. Zhuang, *Proc. Natl. Acad. Sci. U. S. A.*, 2003, **100**, 9280.
7 P. Donoso, M. Beltrán and C. Hidalgo, *Biochemistry*, 1996, **35**, 13419.
8 C. Hunte, E. Screpanti, M. Venturi, A. Rimon, E. Padan and H. Michel, *Nature*, 2005, **435**, 1197.
9 E. R. Chin and D. G. Alllen, *J. Physiol.*, 1998, **512**, 831.
10 B. Tang, F. Yu, P. Li, L. Tong, X. Duan, T. Xie and X. Wang, *J. Am. Chem. Soc.*, 2009, **131**, 3016.
11 H. Izumi, T. Torigoe, H. Ishiguchi, H. Uramoto, Y. Yoshida, M. Tanabe, T. Ise, T. Murakami, T. Yoshida, M. Nomoto and K. Kohno, *Cancer Treat. Rev.*, 2003, **29**, 541.
12 T. A. Davies, R. E. Fine, R. J. Johnson, C. A. Levesque, W. H. Rathbun, K. F. Seetoo, S. J. Smith, G. Strohmeier, L. Volicer, L. Delva and E. R. Simons, *Biochem. Biophys. Res. Commun.*, 1993, **194**, 537.
13 A. Kogot-Levin, M. Zeigler, A. Ornoy and G. Bach, *Pediatr. Res.*, 2009, **65**, 686.
14 D. Ellis and R. C. Thomas, *Nature*, 1976, **262**, 224.
15 S. J. A. Hesse, G. J. G. Ruijter, C. Dijkema and J. Visser, *J. Biotechnol.*, 2000, **77**, 5.
16 R. G. Zhang, S. G. Kelsen and J. C. LaManna, *J. Appl. Physiol.*, 1990, **68**, 1101.
17 F. Han, Y. Xu, D. Jiang, Y. Qin and H. Chen, *Anal. Biochem.*, 2013, **435**, 106.
18 J. Hu, F. Wu, S. Feng, J. Xu, Z. Xu, Y. Chen, T. Tang, X. Weng and X. Zhou, *Sens. Actuators, B*, 2014, **196**, 194.
19 L. Fan, Q. Liu, D. Lu, H. Shi, Y. Yang, Y. Li, C. Dong and S. Shuang, *J. Mater. Chem. B*, 2013, **1**, 4281.
20 Y.-Y. Liu, M. Wu, L.-N. Zhu, X.-Z. Feng and D.-M. Kong, *Chem.–Asian J.*, 2015, **10**, 1304.
21 X.-F. Zhang, T. Zhang, S.-L. Shen, J.-Y. Miao and B.-X. Zhao, *J. Mater. Chem. B*, 2015, **3**, 3260.
22 E. Nakata, Y. Yukimachi, Y. Nazumi, M. Uwate, H. Maseda, Y. Uto, T. Hashimoto, Y. Okamoto, H. Horib and T. Moriia, *RSC Adv.*, 2014, **4**, 348.
23 H. Yu, G. Li, B. Zhang, X. Zhang, Y. Xiao, J. Wang and Y. Song, *Dyes Pigm.*, 2016, **133**, 93.
24 U. C. Saha, K. Dhara, B. Chattopadhyay, S. K. Mandal, S. Mondal, S. Sen, M. Mukherjee, S. V. Smaalen and P. Chattopadhyay, *Org. Lett.*, 2011, **13**, 4510.
25 S. Yao, K. J. Schafer-Hales and K. D. Belfield, *Org. Lett.*, 2007, **9**, 5645.
26 G. Ke, Z. Zhu, W. Wang, Y. Zou, Z. Guan, S. Jia, H. Zhang, X. Wu and C. J. Yang, *ACS Appl. Mater. Interfaces*, 2014, **6**, 15329.
27 S. L. Shen, X. P. Chen, X. F. Zhang, J. Y. Miao, B. X. Zhao, S. Shen, X. Chen, X. Zhang, J. Miao and B. Zhao, *J. Mater. Chem. B*, 2015, **3**, 919.
28 H.-S. Lv, S.-Y. Huang, B.-X. Zhao and J.-Y. Miao, *Anal. Chim. Acta*, 2013, **788**, 177.
29 X.-F. Zhang, T. Zhang, S.-L. Shen, J.-Y. Miao and B.-X. Zhao, *RSC. Adv.*, 2015, **5**, 49115.
30 J. Zhang, M. Yang, C. Li, N. Dorh, F. Xie and F.-T. Luo, *J. Mater. Chem. B*, 2015, **3**, 2173.
31 A. Wallabregue, D. Moreau, P. Sherin, P. M. Lorente, Z. Jarolímová, E. Bakker, E. Vauthey, J. Gruenberg and J. Lacour, *J. Am. Chem. Soc.*, 2016, **138**, 1752.
32 B. Dong, X. Song, C. Wang, X. Kong, Y. Tang and W. Lin, *Anal. Chem.*, 2016, **88**, 4085.
33 X.-L. Shi, G.-J. Mao, X.-B. Zhang, H.-W. Liu, Y.-J. Gong, Y.-X. Wu, L.-Y. Zhou, J. Zhang and W. Tan, *Talanta*, 2014, **130**, 356.
34 Y. Fu, J. Zhang, H. Wang, J.-L. Chen, P. Zhao, G.-R. Chen and X.-P. He, *Dyes Pigm.*, 2016, **133**, 372.
35 G.-J. Song, S.-Y. Bai, X. Dai, X.-Q. Cao and B.-X. Zhao, *RSC Adv.*, 2016, **6**, 41317.
36 L. Fan, S.-Q. Gao, Z.-B. Li, W.-F. Niu, W.-J. Zhang, S.-M. Shuang and C. Dong, *Sens. Actuators, B*, 2015, **221**, 1069.
37 W. Niu, L. Fan, M. Nan, M. S. Wong, S. Shuang and C. Dong, *Sens. Actuators, B*, 2016, **234**, 534.

38 Y. Xu, Z. Jiang, Y. Xiao, F. Z. Bi, J. Y. Miao and B. X. Zhao, *Anal. Chim. Acta*, 2014, **820**, 146.
39 S.-L. Shen, X.-F. Zhang, S.-Y. Bai, J.-Y. Miao and B.-X. Zhao, *RSC Adv.*, 2015, **5**, 13341.
40 W. Niu, L. Fan, M. Nan, Z. Li, D. Lu, M. S. Wong, S. Shuang and C. Dong, *Anal. Chem.*, 2015, **87**, 2788.
41 W.-J. Zhang, L. Fan, Z.-B. Li, T. Ou, H.-J. Zhai, J. Yang, C. Dong and S.-M. Shuang, *Sens. Actuators, B*, 2016, **233**, 566.
42 G. Loving and B. Imperiali, *J. Am. Chem. Soc.*, 2008, **130**, 13630.
43 T. Tanaka and R. Y. Yada, *Arch. Biochem. Biophys.*, 1997, **340**, 355.
44 X. Lin, G. Koelsch, J. A. Loy and J. Tang, *Protein Sci.*, 1995, **4**, 159.
45 X. L. Lin, R. N. Wong and J. Tang, *J. Biol. Chem.*, 1989, **264**, 4482.
46 D. S. Merrell and A. Camilli, *Curr. Opin. Microbiol.*, 2002, **5**, 51.
47 T. A. Krulwich, G. Sachs and E. Padan, *Nat. Rev. Microbiol.*, 2011, **9**, 330.
48 J. W. Foster, *Nat. Rev. Microbiol.*, 2004, **2**, 898.